Vibration Control of Piled-Structures through Structure-Soil-Structure-Interaction

By

Pierfrancesco Cacciola, Maria Garcia Espinosa and Alessandro Tombari

School of Environment and Technology, University of Brighton, Cockcroft Building, Lewes Road, BN24GJ Brighton, UK

ABSTRACT: This paper deals with the vibration control of existing structures forced by earthquake induced ground motion. To this aim it is proposed for the first time to exploit the structure-soil-structure mechanism to develop a device, hosted in the soil but detached from the structure, able to absorb part of the seismic energy so to reduce the vibration of neighbourhood structures. The design of the device is herein addressed to protect monopile structures from earthquake induced ground motion. By modelling the ground motion as zero-mean quasi-stationary response-spectrum-compatible Gaussian stochastic process, the soil as visco-elastic medium and the target monopiled-structure as a linear behaving structure the device, herein called Vibrating Barrier (ViBa), has been designed through an optimization procedure. Various numerical and experimental results are produced to show the effectiveness of the ViBa. Remarkably, a significant reduction of the structural response up to 44% has been achieved.

KEY WORDS: Structure-Soil-Structure-Interaction, vibration control, Ground motion excitation, vibrating barrier, piled-structures.

1 INTRODUCTION

The problem of reducing vibrations in structures, generally known as vibration control, arises in various branches of engineering: civil, aeronautical and mechanical. Unpredicted vibrations can lead to the deterioration or collapse of structures. In the field of earthquake engineering, modern strategies of seismic design aim to reduce structural vibrations by: i) increasing the dissipative properties of the structure; ii) moving the natural frequencies of the structure away from the frequencies in which the seismic action possess the highest energy; iii) modifying the energy transferred from the earthquake to the structure. The control of vibrations of structures is currently performed using passive, active or hybrid strategies. In the framework of passive control systems is it possible to categorize the following three general devices: i) dampers; ii) tuned mass dampers (TMD); iii) isolation systems. Apart from few attempts to protect existing structures the use of vibration control devices is still restricted to new buildings and/or constructions. One main reason is that the introduction of control devices in existing structures is too invasive, costly and requires the demolishing of some structural and/or non-structural components. This is clearly prohibitive for developing countries and for historical buildings. An alternative solution is to protect the structures introducing trenches or sheet-pile walls in the soil (see e.g. Woods [1]). However this approach seems to be more effective for surface waves coming from railways rather than seismic waves. Nevertheless, the use of trenches and more in general devices hosted in the soil appears as an alternative strategy, not yet thoroughly explored to protect structures from earthquakes. Indeed this strategy might be applied to historical buildings as it avoids the demolishing of part of them and also has the potential to be extended to the protection to more than one structure.

Bearing in mind the global necessity to protect existing structures from earthquakes and the limitation of current technologies, a novel control strategy is proposed in this paper.

The basic idea is based on the generally known structure-soil-structure interaction (SSSI) and on the findings from the pioneristic works of Warburton et al. [2] and Luco and Contesse [3].

Specifically, it is know the dynamic structure-soil-structure interaction between two structures occurs through the radiation energy emitted from a vibrating structure to the other structure. As a consequence, the dynamic response of one structure cannot be studied independently from the other one. Warburton et al. [2] studied the dynamic response of two rigid masses in an elastic subspace showing the influence of the presence of one mass in the dynamic response of the other one. Luco and Contesse [3] studied the dynamic interaction between two parallel infinite shear walls placed on rigid foundations and forced by vertically incident SH wave. They showed the interaction effects are especially important for a small shear wall located close to a larger structure. Kobori and Kusakabe [4] extended the structure-soil-structure interaction study to flexible structures and pointed out that the response of a structure might be sensibly smaller due the presence and interaction of another structure. Mulliken and Karabalis [5] evidenced large differences in the response of three adjacent buildings founded on rigid, surface foundations with respect to the single case, by defining a simple discrete model for predicting the dynamic interaction. Effects of both soil-structure interaction and structure-soil-structure interaction were investigated by Naserkhaki and Pourmohammad [6] on response of twin buildings during earthquake excitations. A recent review of the structure-soil-structure interaction problem can be found in Menglin et al. [7]. The natural extension of the traditional structure-soil-structure interaction problem, in which only two structures are considered, is generally known as the site-city interaction problem. Due to the difficulties involved in modelling the multiple interactions and the sustained progress in computational mechanics, numerical approaches based on wave propagation and finite or boundary element analysis are usually adopted for the study of site-city interaction [8-10].

Interestingly in [10] it has been shown as the energy of ground motion at the free field in the city might be reduced by around 50% due to the perturbation induced by resonant buildings. Analytical studies on site-city interaction have also been proposed in the literature by Guéguen et al. [11] and Boutin and Roussillon [12]. In [11] the effect of the city is accounted for by modelling the structures

as simple oscillators, while in [12] the multiple interactions between buildings are studied through homogenization methods.

The SSSI study is generally dealt with through a deterministic approach and few attempts have been made to consider seismic action as a random process. In the framework of the stochastic seismic analysis of the structure-soil-structure interaction problem Behnamfar and Sugimura [13] performed a parametric study of a 2D system consisting of two structures connected to a homogeneous, visco-elastic medium resting over a half-space by considering P-, SV-and Rayleigh wave propagation modelled as a stationary process. Alexander et al. [14] recently developed a discrete model to study the SSSI problem in the case of both deterministic and stochastic ground motion excitation.

Although it has been observed in the past by several authors the beneficial effect of the presence of a structure to reduce the vibrations of another this interaction has not been yet used, to the best knowledge of the authors, as a tool for the seismic vibration control. In this paper it is proposed for the first time to design a structural system, herein called Vibrating Barrier (ViBa), to reduce the vibration of a neighborough structure. The ViBa is designed in this paper to control the vibrations of pile-structures. To this aim, in order to better exploit the SSSI, the ViBa-soil-structure interaction model is developed by designing the ViBa as a piled structure as well. The numerical model used for describing the overall system has been derived by extending the approach used by several authors (Dobry and Gazetas [15], Mylonakys and Gazetas [16], Makris and Gazetas [17] and Dezi et al. [18]) for pile group foundations in order to simulate the ViBa-soil-structure interaction problem. In this approach, the soil is assumed as a Winkler-type medium, that is composed as a set of independent horizontal soil layers. The pile–soil–pile interaction effect and the radiation problem of the waves towards infinity are accounted for by means of complex impedances derived from elastodynamic Green’s functions.

Furthermore the stochastic analysis of the ViBa-soil-structure interaction problem is performed. The structure and the ViBa are both modelled as linear behaving systems, the soil as a visco-elastic medium and the ground motion excitation as a zero-mean response-spectrum compatible Gaussian stationary/quasi stationary process. According to this hypothesis the structural parameters of the ViBa are optimized so to reduce a prefixed fractile of the maximum response of the target structure. Numerical and experimental results showed a remarkable reduction of the response up to 44% in terms of maximum relative displacement.

2 PROBLEM FORMULATION

Consider the ViBa-soil-structure system illustrated in Figure 1. In agreement with traditional vibration control strategies and structure-soil-structure interaction studies (see e.g. [14]) simplified models will be adopted in this paper to study the ViBa-soil-structure problem. Specifically the system consists of a cantilevered structure to be protected and the ViBa both assumed linear behaving and supported by monopile foundations. The soil is assumed to be a linear visco-elastic medium.

In order to analyse the mutual interaction between ViBa and structure, the general problem is discretized in n_e elements and n_J joints as depicted in Figure 2. For simplicity's sake vertical displacements are neglected and masses are assumed as lumped, therefore every joint possesses two degrees of freedom. Due to the visco-elastic model adopted for the soil the equations of motion of the ViBa-soil-structure interaction model in terms of absolute displacements is cast in the frequency domain as follows:

$$\left(\widetilde{\mathbf{K}}(\omega) - \omega^2\mathbf{M}\right)\mathbf{U}(\omega) = \mathbf{F}(\omega) \tag{1}$$

where $\mathbf{M}$ is the real [n x n] diagonal global mass matrix, $\widetilde{\mathbf{K}}(\omega)$ is the complex [n x n] global stiffness matrix, $\mathbf{U}(\omega)$ is the [n x 1] vector of the frequency Fourier transform of the nodal absolute

displacements and $\mathbf{F}(\omega)$ is the [n x 1] vector of the frequency Fourier transform of the nodal forces and *n* is the number of the degrees of freedoms. By ordering the vector $\mathbf{U}(\omega)$ as follows

$$\mathbf{U}(\omega)=\begin{Bmatrix}\mathbf{U}_{S,1}(\omega)\\ \mathbf{U}_{F,1}(\omega)\\ \mathbf{U}_{F,2}(\omega)\\ \mathbf{U}_{S,2}(\omega)\end{Bmatrix} \tag{2}$$

where $\mathbf{U}_{S,i}$ and $\mathbf{U}_{F,i}(\omega)$ (i=1,2) are the vector collecting the absolute displacements of the structure and of the foundation respectively, Equation 1 can be rewritten in extended form in the following way:

$$\left(\begin{bmatrix}\widetilde{\mathbf{K}}_{SS,1} & \widetilde{\mathbf{K}}_{SF,1} & 0 & 0\\ \widetilde{\mathbf{K}}_{FS,1} & \widetilde{\mathbf{K}}_{FF,1}(\omega) & \widetilde{\mathbf{K}}_{FF,c}(\omega) & 0\\ 0 & \widetilde{\mathbf{K}}_{FF,c}(\omega) & \widetilde{\mathbf{K}}_{FF,2}(\omega) & \widetilde{\mathbf{K}}_{FS,2}\\ 0 & 0 & \widetilde{\mathbf{K}}_{SF,2} & \widetilde{\mathbf{K}}_{SS,2}\end{bmatrix} - \omega^2\begin{bmatrix}\mathbf{M}_{SS,1} & 0 & 0 & 0\\ 0 & \mathbf{M}_{FF,1} & 0 & 0\\ 0 & 0 & \mathbf{M}_{FF,2} & 0\\ 0 & 0 & 0 & \mathbf{M}_{SS,2}\end{bmatrix}\right)\begin{Bmatrix}\mathbf{U}_{S,1}(\omega)\\ \mathbf{U}_{F,1}(\omega)\\ \mathbf{U}_{F,2}(\omega)\\ \mathbf{U}_{S,2}(\omega)\end{Bmatrix} = \begin{Bmatrix}0\\ \mathbf{F}_{F,1}(\omega)\\ \mathbf{F}_{F,2}(\omega)\\ 0\end{Bmatrix} \tag{3}$$

where $[\cdot]_{SS,i}$ and $[\cdot]_{FF,i}$ indicates the sub matrices related to the superstructure and the soil-foundation sub system, respectively and $[\cdot]_{SF,i}$ and $[\cdot]_{FS,i}$ refers to the coupling between the superstructure and the foundation (for i =1,2). Furthermore $[\cdot]_{FF,c}$ is referred to the structure-soil-structure interaction effects, namely it indicates the coupling between the foundations of the two structures. Hysteretic damping [19] is used in the analysis to model the dissipation of energy in both the soil and the structures, therefore all the stiffness sub-matrices in Equation 2 can be written as

$$\widetilde{\mathbf{K}}_{rs,i} = \mathbf{K}_{rs,i}(1 + j\eta_{rs,i}) \quad (i=1,2; \quad r=F,S; \; s=F,S) \tag{4}$$

where $\eta_{rs,i}$ is the loss factor and $j = \sqrt{-1}$ is the imaginary unit. In Equation 3, $\widetilde{\mathbf{K}}_{FF,i}(\omega)$ is the [m $\times$ m] stiffness matrix of the pile and it is given by the sum of the stiffness matrix of the pile structure $\mathbf{K}_{FF,i}^{pile}$ and the diagonal matrix of the visco-elastic soil $\mathbf{K}_{FF}^{soil}(\omega)$, that is

$$\widetilde{\mathbf{K}}_{FF,i}(\omega) = \widetilde{\mathbf{K}}_{FF,i}^{pile} + \widetilde{\mathbf{K}}_{FF}^{soil}(\omega) \tag{5}$$

where $\widetilde{\mathbf{K}}_{FF,i}^{pile}$ is determined through the traditional Finite Element approach by considering Euler-Bernoulli beam elements whereas $\widetilde{\mathbf{K}}_{FF}^{soil}(\omega)$ takes into account to the contribution of both soil-structure-interaction (SSI) and coupling between the two structures, i.e. the structure-soil-structure-interaction and in accordance with the Winkler type model depicted in Figure 2 it is derived as $\widetilde{\mathbf{K}}_{FF}^{soil}(\omega) = diag\left[\dots, k_{FF}^{SSI}(z_i, \omega) + k_{FF}^{SSSI}(z_i, \omega), \dots\right]$. It has to be emphasized that the number of joints in both structures 1 and 2 are the same so to facilitate the SSSI modelling. Note also that in Equation (5) the dependency by the circular frequency ω is due to the additional geometrical dissipation of energy generally known as radiation damping.

To determine the values of both $k_{FF}^{SSI}(z, \omega)$ and the $k_{FF}^{SSSI}(z, \omega)$, in this paper, the procedure proposed by Dobry and Gazetas [15] for floating pile groups has been extended to evaluate the dynamic stiffness and damping of the foundations for the case in which SSSI effects are involved. As first step, the dynamic soil response of single pile subjected to dynamic load obtained by Novak [20] under the hypothesis of plane strain conditions and embedded in a homogeneous, isotropic soil medium has been assumed. Therefore, the dynamic horizontal reaction of a rigid, massless, circular cylinder of radius *r* and height dz, is thus evaluated by the following expression:

$$k_{FF}(z, \omega) = 2\pi G(z) a_0 \frac{\frac{1}{\sqrt{q}} \cdot H_2^2(a_0)H_1^2(x_0) + H_2^2(x_0)H_1^2(a_0)}{H_0^2(a_0)H_2^2(x_0) + H_0^2(x_0)H_2^2(a_0)} dz \tag{6}$$

where $q = \frac{1-2\nu}{2(1-\nu)}$, $x_0(z) = a_0(z)\sqrt{q}$, ν is the Poisson's ratio, $a_0(z) = \frac{\omega r}{V_s(z)}$, H_i^2 is the Hankel function of the second kind of order *i*, $G(z)$ the shear modulus at depth z and assumed constant in the interval [z-dz/2, z+dz/2], and $V_s(z)$ is the shear wave velocity of the considered soil layer at depth z. Note that the dependence of $x_0(z)$ and $a_0(z)$ from the depth z in Equation (6) is omitted for brevity sake. In order to calibrate the dynamic stiffness $k_{FF}^{SSI}(z, \omega)$ related to the vibration of the single pile

and the dynamic stiffness k_{FF}^{SSSI} representing the coupling interaction due to the propagation of the vibrations arising from each structure and traveling through the soil, the attenuation function proposed by Dobry and Gazetas [15] is herein used to analyse the SSSI problem. The attenuation function $\alpha(S,\omega)$ is necessary to obtain the displacement field around a vibrating foundation at a distance S. From the acoustic theory, Morse and Ingard [21] obtained the following relation for asymptotic cylindrical waves propagating from a cylinder subjected to harmonic force:

$$U(S,\omega) \cong \frac{A}{\sqrt{S}} \exp\left(-\frac{\eta\omega S}{V_{La}}\right) \exp\left[-j\omega\left(t-\frac{S}{V_{La}}\right)\right] \tag{7}$$

where S is the spacing between source and receiver pile, t is the time, A is the amplitude of wave oscillation and η is the hysteretic damping ratio of the soil, $V_{La} = (3.4V_s)/[\pi(1-\nu)]$ is the Lysmer's analogue velocity used when the alignment of the piles is in the same direction of the propagation of the travelling waves.

Moreover, the displacement of the pile under its own dynamic load is obtained from (6):

$$U(r,\omega) \cong \frac{A}{\sqrt{r}} \cdot \exp(j\omega t) \tag{8}$$

where it is assumed that there is not time lag ($V_{La} \to \infty$) between the pile axis and its perimeter. Therefore, the attenuation $\alpha(S,\omega)$ yields

$$\alpha(r,S,\omega) = \frac{U(S,\omega)}{U(r,\omega)} = \sqrt{\frac{r}{S}} \exp\left(-\frac{\eta\omega S}{V_{La}}\right) \exp\left[-j\omega\left(\frac{S}{V_{La}}\right)\right] \tag{9}$$

This expression allows computing the effect on the receiver pile once the behaviour single pile is obtained. Therefore, the displacements of the piles i=1 and i=2 under harmonic forces $[F_1 \quad F_2]$ are obtained by superposition of the two contributions at the same depth z: $U_{ii}(z,\omega)$ and $U_{kk}(z,\omega)\alpha(r_k,S,\omega)$; $(i=1,2; k=1,2)$ related to the displacement of the single pile and to the influence of the second pile on the first pile, respectively. Therefore, the equations of the displacements of a generic joint of the two piles at depth z are written as follows:

$$\begin{aligned} \mathrm{U}_1(\mathrm{z},\mathrm{S},\omega) &= \mathrm{U}_{11}(\mathrm{z},\omega) + \mathrm{U}_{22}(\mathrm{z},\omega)\alpha(\mathrm{r}_2,\mathrm{S},\omega) \\ \mathrm{U}_2(\mathrm{z},\mathrm{S},\omega) &= \mathrm{U}_{22}(\mathrm{z},\omega) + \mathrm{U}_{11}(\mathrm{z},\omega)\alpha(\mathrm{r}_1,\mathrm{S},\omega) \end{aligned} \tag{10}$$

Eq. (10) constitutes a strategy to define an equivalent spring linear model ensuring the same displacements of Eq. (10) at each depth z_i (Dobry and Gazetas [15]). By assuming $\mathrm{u}_{ii} = F_i/\mathrm{k}_{\mathrm{FF}}$ and setting for simplicity's sake $\mathrm{r} = r_1 = r_2$, Eq. (10) can be restated as

$$\frac{1}{\mathrm{k}_{\mathrm{FF}}}\begin{bmatrix} 1 & \alpha(\mathrm{r},\mathrm{S},\omega) \\ \alpha(\mathrm{r},\mathrm{S},\omega) & 1 \end{bmatrix}\begin{bmatrix} F_1 \\ F_2 \end{bmatrix} = \begin{bmatrix} \mathrm{U}_1(\mathrm{r},\mathrm{S},\omega) \\ \mathrm{U}_2(\mathrm{r},\mathrm{S},\omega) \end{bmatrix} \tag{11}$$

Therefore,

$$\frac{\mathrm{k}_{\mathrm{FF}}}{[1-\alpha^2(\mathrm{r},\mathrm{S},\omega)]}\begin{bmatrix} 1 & -\alpha(\mathrm{r},\mathrm{S},\omega) \\ -\alpha(\mathrm{r},\mathrm{S},\omega) & 1 \end{bmatrix}\begin{bmatrix} \mathrm{U}_1 \\ \mathrm{U}_2 \end{bmatrix} = \begin{bmatrix} F_1 \\ F_2 \end{bmatrix} \tag{12}$$

Note that the first element of the equivalent stiffness matrix in Equation (12) is given by the superposition of the stiffness of the two springs $\mathrm{k}_{\mathrm{FF}}^{\mathrm{SSI}}$ and the $\mathrm{k}_{\mathrm{FF}}^{\mathrm{SSSI}}$ placed in series as shown in the reference model in Figure 2, while the off diagonal terms represent directly the term $\mathrm{k}_{\mathrm{FF}}^{\mathrm{SSSI}}$. Therefore after simple algebra they are determined as follows:

$$\mathrm{k}_{\mathrm{FF}}^{\mathrm{SSI}}(z_i,\omega) = \mathrm{k}_{\mathrm{FF}}(z_i,\omega)[1+\alpha(\mathrm{r},\mathrm{S},\omega)]^{-1} \tag{13}$$

and

$$\mathrm{k}_{\mathrm{FF}}^{\mathrm{SSSI}}(z_i,\omega) = \mathrm{k}_{\mathrm{FF}}(z_i,\omega)\frac{\alpha(\mathrm{r},\mathrm{S},\omega)}{[1-\alpha^2(\mathrm{r},\mathrm{S},\omega)]} \tag{14}$$

It is worth noting that in case of uncoupled case (i.e. $\mathrm{S} \to \infty$), the attenuation function α assumes the null value and the expression (6) for the single pile is again obtained ($\mathrm{k}_{\mathrm{FF}}^{\mathrm{SSI}} \to \mathrm{k}_{\mathrm{FF}}$) while the coupling term $\mathrm{k}_{\mathrm{FF}}^{\mathrm{SSSI}}$ is zero.

The matrix $\mathbf{K}_{\mathrm{FF,c}}(\omega)$ lists the coupling terms given by Equation (14) as $\mathbf{K}_{\mathrm{FF,c}}(\omega) = diag\left[\dots, \mathrm{k}_{\mathrm{FF}}^{\mathrm{SSSI}}(z_i,\omega), \dots\right]$ and the matrices $\widetilde{\mathbf{K}}_{\mathrm{FS,i}}$ and $\widetilde{\mathbf{K}}_{\mathrm{SF,i}}(i = 1,2)$ are determined through traditional assembling FE procedures and list the coupling terms between the *i*th structure and its

foundation. Moreover, the nodal forces $\mathbf{F}(\omega)$ are determined through the seismic wave propagation of shear waves from the bedrock through the soil deposit as

$$\mathbf{F}(\omega) = \mathbf{Q}(\omega)\mathbf{H}_{\text{soil}}(\omega)\mathrm{U}_{\mathrm{g}}(\omega) \tag{15}$$

where $\mathbf{H}_{\text{soil}}(\omega)$ is the $[2\mathrm{m} \times 1]$ vector listing the transfer functions of the soil deposit at the depth z_i, $\mathrm{U}_{\mathrm{g}}(\omega)$ is the Fourier transform of the ground motion displacement at the bedrock and $\mathbf{Q}(\omega)$ is the $[\mathrm{n} \times 2\mathrm{m}]$ matrix defined as:

$$\mathbf{Q}(\omega) = \begin{bmatrix} 0 & 0 \\ \widetilde{\mathbf{K}}^{\mathrm{SSI}}_{\mathrm{FF},1}(\omega) & 0 \\ 0 & \widetilde{\mathbf{K}}^{\mathrm{SSI}}_{\mathrm{FF},2}(\omega) \\ 0 & 0 \end{bmatrix} \tag{16}$$

where $\widetilde{\mathbf{K}}^{\mathrm{SSI}}_{\mathrm{FF,i}}(\omega)$ is a diagonal matrix listing the stiffness $\mathrm{k}^{\mathrm{SSI}}_{\mathrm{FF}}(z_i, \omega)$ connected to the joints of the piles. It is noted that ground motion acceleration is considered the same at the bedrock underneath both structure and device. Ground motion horizontal propagation can be also included in the formulation by the meaning of the vector $\mathbf{U}_{\mathrm{g}}(\omega)$ taking into account wave propagation and incoherent effects. For sake of simplicity horizontal propagation will be omitted in this paper.

3 STOCHASTIC RESPONSE AND VIBA DESIGN

Consider the ViBa-soil-structure system is forced by a ground motion excitation determined through the propagation of the seismic wave from the bedrock to the ground surface. The ground motion at the bedrock is modelled by a Gaussian monocorrelated zero-mean stationary process defined by the power spectral density function (PSD) of the ground displacement $\mathrm{G}_{\mathrm{U_gU_g}}(\omega)$. The stochastic structural response is determined as:

$$\mathrm{E}[\mathbf{U}(\omega)\mathbf{U}^{*}(\omega)] \tag{17}$$
$$= \mathrm{E}\left[\left(\widetilde{\mathbf{K}}^{-1}{}_{\mathrm{dyn}}(\omega)\mathbf{Q}(\omega)\mathbf{H}_{\text{soil}}(\omega)\right)\left(\widetilde{\mathbf{K}}^{-1}{}_{\mathrm{dyn}}(\omega)\mathbf{Q}(\omega)\mathbf{H}_{\text{soil}}(\omega)\right)^{*}\right]\mathrm{G}_{\mathrm{U_gU_g}}(\omega)$$

where $*$ is the complex conjugate transpose, $\mathrm{E}[\cdot]$ is the expectation operator, and $\widetilde{\mathbf{K}}_{\mathrm{dyn}} = \widetilde{\mathbf{K}}(\omega) - \omega^2\mathbf{M}$; therefore after setting $\mathbf{H}_{\mathrm{glob}}(\omega) = \widetilde{\mathbf{K}}^{-1}{}_{\mathrm{dyn}}(\omega)\mathbf{Q}(\omega)\mathbf{H}_{\mathrm{soil}}(\omega)$, Equation (17) yields

$$\mathbf{G}_{\mathrm{UU}}(\omega) = \mathbf{H}_{\mathrm{glob}}(\omega)\mathbf{H}^{*}_{\mathrm{glob}}(\omega)\mathrm{G}_{\mathrm{U_gU_g}}(\omega) \tag{18}$$

where $\mathbf{G}_{\mathrm{UU}}(\omega)$ is the PSD matrix of the response in terms of absolute displacements. Moreover, the fractile of order p of the distribution of maxima of the relative horizontal displacements U_r of the structure to be protected is determined through the first crossing problem:

$$\mathrm{X}_{Ur}(Ts, p) = \eta_{Ur}(Ts, p)\sqrt{\lambda_{0,Ur}} \tag{19}$$

where Ts is the time observing window; η_{Ur} is the peak factor; $\lambda_{0,Ur}$ is the zero-order response spectral moment. The peak factor determined by Vanmarcke [22] is used:

$$\eta_{Ur}(Ts, p) = \sqrt{2\ln\left\{2N_{Ur}\left[1 - \exp\left[-\delta_{Ur}^{1.2}\sqrt{\pi\ln(2N_{Ur})}\right]\right]\right\}} \tag{20}$$

with

$$N_{Ur} = \frac{T_S}{-2\pi\ln p}\sqrt{\frac{\lambda_{2,Ur}}{\lambda_{0,Ur}}} \tag{21}$$

and

$$\delta_{Ur} = \sqrt{1 - \frac{\lambda_{1,Ur}^2}{\lambda_{0,Ur}\lambda_{2,Ur}}} \tag{22}$$

where the response spectral moments $\lambda_{i,Ur}$ are given by the following equation:

$$\lambda_{i,Ur} = \int_0^{+\infty} \omega^i \mathrm{G}_{UrUr}(\omega)d\omega \tag{23}$$

$\mathrm{G}_{UrUr}(\omega)$ is the PSD function of the horizontal relative displacements between the absolute top displacement of the structure and the foundation; it can be obtained by the following relation:

$$\mathrm{G}_{UrUr}(\omega) = \mathrm{G}_{U_TU_T}(\omega) + \mathrm{G}_{U_FU_F}(\omega) - \mathrm{G}_{U_TU_F}(\omega) - \mathrm{G}_{U_FU_T}(\omega) \tag{24}$$

where the subscripts U_T and U_F are the absolute top displacement of the structure and the absolute top displacement of the foundation, respectively. Note that the PSD matrix of the response (see e.q. 18) lists both the response of the ViBa and of the structure to be protected. Therefore it can be used as vehicle to minimize the maximum response statistics by calibrating the ViBa structural parameters as shown in the next section.

The optimal dynamic characteristics of the ViBa designed to reduce the vibrations of adjacent structures under stochastic seismic load are determined in this section. The optimization procedure aims to reduce a target response parameter selected by the designer. In the following the relative displacement of the structure to be protected is selected as representative, even though different response parameter can be chosen to define alternative penalty functions. According to the modelling adopted to describe the ViBa-soil-structure interaction, the design parameters of the ViBa device are the internal mass $\mathbf{M}_{\mathrm{SS},1}$, the stiffness $\mathbf{K}_{\mathrm{SS},1}$ and the damping $\eta_{ss,1}$. In order to reduce the maximum relative displacements expressed by first passage problem in Equation (19), the power spectral density function (18) is restated by introducing the vector $\boldsymbol{\beta} = \left[\mathbf{M}_{\mathrm{SS},1}; \mathbf{K}_{\mathrm{SS},1}; \eta_{ss,1}\right]$ listing the design parameters as follows:

$$\mathbf{G}_{\mathrm{UU}}(\omega, \boldsymbol{\beta}) = \mathbf{H}_{\mathrm{glob}}(\omega, \boldsymbol{\beta})\mathbf{H}^{*}_{\mathrm{glob}}(\omega, \boldsymbol{\beta})\mathrm{G}_{\mathrm{U_g U_g}}(\omega) \tag{25}$$

where $\mathbf{H}_{\mathrm{glob}}(\omega) = \widetilde{\mathbf{K}}^{-1}{}_{\mathrm{dyn}}(\omega, \boldsymbol{\beta})\mathbf{Q}(\omega)\mathbf{H}_{\mathrm{soil}}(\omega)$.

Therefore the optimization procedure aims to minimize the largest value of the peak of the relative horizontal displacements of the structure at the not-exceeding probability p as follows:

$$min\left\{\mathrm{X}_{Ur}(Ts, p, \boldsymbol{\beta}) = \eta_{Ur}(Ts, p, \boldsymbol{\beta})\sqrt{\lambda_{0,Ur}(\boldsymbol{\beta})}\right\}, \qquad \boldsymbol{\beta}_{min} < \boldsymbol{\beta} < \boldsymbol{\beta}_{max} \tag{26}$$

It is worth noting that the optimization procedure is bounded to control each parameter of the vector $\boldsymbol{\beta}$ achieving physically reliable values at each iteration.

4 NUMERICAL ANALYSES

4.1 Case studies

In this section the previous procedure is applied to obtain the ViBa parameters in order to minimize the relative displacement response of the monopile structure depicted in Figure 1. The structure is 12.5m tall of which 10 m is embedded on the ground working as pile foundation whereas the part over the ground surface is H_p= 2.5 m. The shaft is made in reinforced concrete with circular section of 1 meter radius. A lumped mass of 500.000 kg is placed on the top of the structure. Hysteretic-type damping assumed fixed at 0.1 is considered. The ViBa is modelled as the structure: the foundation is a 10 meter depth monopile with the same diameter of the structure to be protected. The mass, the height and the hysteretic damping factor of the ViBa will be the design parameters calibrated to minimize the response of the target structure.

Both structures and ViBa are founded on a 30 meter thickness deposit. The soil is considered as a homogeneous linear visco-elastic material. Several shear wave velocities, as reported in Table 1, are investigated in the analysis in order to study the response for the soil types described by seismic design codes (see e.g. [23]).

4.2 Determination of the input PSD

In this section, the 1D linear site response analysis is carried out for capturing the local site effects for each of the investigated soil deposits. By performing a steady state analysis, the transfer functions $\mathbf{H}_{\mathrm{soil}}(\omega)$ are evaluated in order to determine the free field motion displacement at each depth in which the pile is discretized. Therefore, from Equation (18), the stationary power spectral density function of the ground displacement $G_{U_g U_g}(\omega)$ used in this analysis is determined from the response-spectrum-compatible model obtained for the ground motion acceleration by Cacciola et al. [24]. Specifically,

$$G_{\ddot{U}_g\ddot{U}_g}(\omega_i) = \frac{4\zeta_0}{\omega_i\pi - 4\zeta_0\omega_{i-1}}\left(\frac{RSA(\omega_i,\zeta_0)^2}{\eta_u^2(\omega_i,\zeta_0)} - \Delta\omega\sum_{k=1}^{i-1} G_{\ddot{U}_g\ddot{U}_g}(\omega_i)\right) \tag{27}$$

where η_u is the peak factor given in Equation 15 with N_U and δ_U given by the following equations:

$$N_U = \frac{T_S}{-2\pi\ln p}\omega_i \tag{28}$$

and

$$\delta_U = \left[1 - \frac{1}{1-\zeta_0^2}\left(1 - \frac{2}{\pi}\arctan\frac{\zeta_0}{1-\zeta_0^2}\right)^2\right]^{1/2} \tag{29}$$

Moreover, $G_{\ddot{U}_g\ddot{U}_g}(\omega_i < \omega_a) = 0$ where $\omega_a \cong 1\ rad/s$ is the lowest bound of the existence domain of η_u and $RSA(\omega_i,\zeta_0)$ is the response spectral acceleration consistent with the bedrock classified as soil type A according to Eurocode 8 [23]. Figure 3 shows the input PSD of the ground motion acceleration used in the analysis for damping ratio $\zeta_0 = 0.05$ and $T_S = 20s$. Therefore the power spectral density function of the ground motion displacement is $G_{U_gU_g}(\omega) = G_{\ddot{U}_g\ddot{U}_g}(\omega)/\omega^4$.

4.3 Numerical results

This section presents the numerical results of the case study previously described in section 5.1. A parametric study is initially conducted varying the mass m_{ViBa} of the ViBa between 0.25 to 2 times the mass m_{str} of the structure to be protected. Moreover, the stiffness and the damping of the ViBa are selected as parameters of optimization procedure by means of the vector $\boldsymbol{\beta} = [K_{SS,1}; \eta_{ss,1}]$ in which the stiffness $K_{SS,1}$ is equal to $3\,E_{ViBa}J_{ViBa}/H_{ViBa}{}^3$ where $E_{ViBa} = 30000$ MPa is the Young's modulus of the concrete and J_{ViBa} is the moment of inertia of the circular shaft. Accordingly, the optimal parameters are the height H_{ViBa} and the hysteretic damping $\eta_{ss,1}$ of the ViBa and they are both evaluated for each of the several pile-pile spacing considered in the analysis. Lower bound of the hysteretic damping, $\eta_{ss,1}$, has been set equal to 0.02 according to engineering considerations

even though beneficial effects might be occur for lower values of damping. The analyses are carried out for each of the soil deposit reported in Table 1.

Numerical results are illustrated in terms of reduction factor RF defined as:

$$\mathrm{RF} = \frac{X_{\mathrm{U}_{Ur}^{coupled}}}{X_{\mathrm{U}_{Ur}^{uncoupled}}} \tag{30}$$

where $X_{\mathrm{U}_{Ur}^{coupled}}$ and $X_{\mathrm{U}_{Ur}^{uncoupled}}$ are the median values of the peak (i.e. p = 0.5) obtained by Equation (14) of the relative displacements of the structure coupled and uncoupled with the ViBa, respectively.

Figure 4 shows the reduction factor curves for the several soil types obtained for assigned mass ratios by varying the spacing between the structure and the ViBa. Each marker is determined by independent optimization of the ViBa. Clearly, the higher the RF value the lower is the efficiency of the ViBa. A value of the RF greater than 1 denotes a detrimental effect of the ViBa on the structural response. Also the RF values will be higher as the distance between the ViBa and structure increases. Nevertheless, a reduction of around 20%, RF= 0.83, is achieved for the case related to the soil type C at long distance (50 m) when the mass of the ViBa is high (i.e. 2 times the mass of the structure).

It is worth noting that the RF assumes small values at spacing less than 10 meters; it proves the high efficacy of the ViBa for engineering practical distances. The best case is achieved for the case of soil type C, with the higher mass and closest spacing in which the obtained RF is 0.56, which is a 44% of reduction compared to the case of uncoupled structure.

By focusing on the case related to the spacing = 1 m, Figure 5 shows the RF curves for each soil type on varying the mass ratio. Additionally, a comparison with the results obtained from a Monte Carlo Simulation (MCS) performed in the frequency domain by using 100 quasi-stationary samples generated by the meaning of the power spectral density function of Figure 3, is carried out. The excellent matching between the time and frequency domain solutions further validates the accuracy of the formulation adopted.

The curves show that the efficiency of the ViBa increases with the increase of the mass ratio. Moreover, the RF curves are different for each soil type and the smallest RFs are obtained for the soil type C. One cause can be elicited from Table 2 that lists the first fundamental frequencies (in Hz) of the soil deposit and the uncoupled single structure for each soil type; the smaller is the difference between the natural frequency of the soil and the natural frequency of the structure the higher is the efficiency of the ViBa, namely the smaller is the RF. Indeed, when the two natural frequencies are closer each other, the structure is in the situation referred to as double resonance and the displacements of the uncoupled structure are significantly high; the protection provided from the ViBa considerably decreases the structural relative displacement by absorbing a significant part of the seismic input energy.

Figure 6 shows the effects of the ViBa with the distance. The ViBa has been optimized for the spacing = 1 m and its effects are sensible as far as around 120 m where the curves become asymptotic to the unity where the structure to be protected is no more affected by the coupling interaction with the ViBa.

Figure 7 shows the PSD functions of the response acceleration $G_{\ddot{U}_T\ddot{U}_T}(\omega) = \omega^4 G_{U_T U_T}(\omega)$ for the soil types adopted in this paper obtained for the case of mass ratio = 0.75 and pile-pile spacing = 1 m. The continuous line is related to the PSD in term of absolute acceleration of the response of the structure after being protected by the ViBa; the dotted line is related to the same response before being protected by ViBa (uncoupled case). The highest reduction is obtained for the case related to the soil type C where the structure is in resonance with the ground motion excitation due to the natural frequency of the soil deposit; in this case the ViBa is able to reduce of about 40% the maximum absolute acceleration.

A relevant reduction is achieved also for the case in the soil type D, where the difference between the natural frequency of the soil and of the structure is moderate. Moreover, the highest peak is

related to the frequency of the soil deposit (0.83 Hz) whereas in the other cases the highest peaks are consistent with the frequency of the structure to be protected.

It is worth noting that in every case the PSD of the coupled case shows a further peak with regards to the uncoupled case; this is due to the influence of the ViBa that produce the typical shape of the Tuned Mass Damper. A similar behaviour has been observed in the past see e.g. Luco and Contesse [3], Kobori and Kusakabe [4], and more recently by Alexander et al. [12] in the case of the study of cross dynamic interaction of structures founded on surface foundations and by Padròn et al. [25] in the case of nearby pile supported structures as well as in the laboratory and field tests on models of nuclear power plant buildings conducted by the Nuclear Power Electric Corporation (NUPEC) for investigating the dynamic cross interaction effects [26-27]. Figure 8 illustrates the stochastic response of the internal unit of the ViBa under the same input and soil profiles used for Figure 7. The Figure shows the increment of the energy absorbed by the device in comparison with the uncoupled case that can be used to ensure the designed ViBa does not collapse under seismic action.

5 LABORATORY TEST

In this section the effectiveness of the ViBa is evaluated by means of laboratory tests. The study case involves the protection of a structure modelled as cantilevered structure founded on monopile foundation as well as the designed ViBa. The test model consists of a ground model made of silicone rubber and structural models made of steel for the superstructure and aluminium for the pile shaft. Structural models are founded on the ground model with their piles embedded in the silicone rubber specimen (see e.g. Kitada et al. [26] and Niwa et al.[28]). Two cases are analysed: firstly, the case related to the single structure, specifically the uncoupled situation without the protection by the ViBa and secondly the case of the structure with the vibration control provided by the ViBa. The test model is set up on a reduced scale shaking table. The two test models are depicted in Figure 9a-b for both the cases uncoupled and coupled with the ViBa. An Experimental Monte Carlo Simulation

(EMCS) is applied to the test model in order to investigate the reduction of the response acceleration at the top of the structure induced by the ViBa.

5.1 Test set-up

Figure 10 shows the set-up of the experimental test. The ground model has been reproduced by a cylinder made of silicone rubber depicted in Figure 9a-b. The structure is composed of 3-mm diameter steel bar of 0.125 m net height with a 73.2 gr mass placed at the top of the shaft. The shaft is fixed to the single pile foundation made of aluminium. The pile shaft has dimensions of 6 mm in diameter and 0.1 m in length. The elastic properties of the materials used in the test are reported in Table 3. The pile is fixed into the silicon rubber except for a part of 0.03 m length kept above the surface to allow the setting of the transducers. The same structural system has been used for modelling the ViBa where the net height of the pier shaft is obtained according to the procedure defined in Section 3.1. The ViBa is placed at the interaxial distance of 0.05 m between the two piles. The test model is set up on Quanser Shake Table II for performing dynamic tests with simulated earthquake ground motion accelerations. An accelerometer is mounted on the shake table platform in order to measure directly the accelerations at the base of the test model and an accelerometer of 4.2 gr is mounted on the upper mass of the structure in order to record the structural response of the structure to be protected. Monte Carlo Simulation has been performed experimentally. In particular, 30 quasi-stationary ground motion time-histories were generated by using the power spectral density function of Figure 3 adopted in the numerical analyses.

5.2 ViBa design

In this test the ViBa parameter to be designed is the net height of the pier shaft directly related to the ViBa stiffness while the mass of the device is set as almost twice of that one of the structure ($\mathrm{m_{ViBa}} = 174.8\, gr$). In this experimental test, the reduction factor involved in the optimization procedure described in Section 3.1 is expressed in terms of ratio of the absolute accelerations

measured by the accelerometer directly mounted on the top of the structure. Along with the reference model, the test model has been reproduced in SAP2000 [29]. The numerical model is used for simulating the actual boundary conditions of the experimental test that might differ from the ideal model described in the previous section possessing boundary at infinity; the model has been used for calibrating an equivalent hysteretic-type damping used for the ViBa design and equal to $\eta = 0.09$. Both cases of single structure and structure protected by the ViBa device are carried out by means of the models depicted in Figure 11a and b, respectively. The silicone rubber ground model, the piles and the piers of both structure and ViBa are modelled by means of solid elements. Power spectral density analyses have been performed by applying the PSD functions recorded at the shaking table platform. Results are then compared to those obtained by the experimental tests in order to better calibrate the hysteretic damping of the system. Consequently by setting up the reference model, the outcome of the procedure has resulted in a net height of 0.08 m for which the achieved reduction factor is 0.78.

5.3 Shaking table results

Shaking table tests are carried out for 30 simulated ground motion accelerations for both cases of single structure and structure protected by the ViBa. The results of the experimental Monte Carlo Simulation are the structural accelerations recorded at the top of the structure. Figure 12 shows the target PSD function used for generating the accelerograms and the PSD curves obtained by averaging each PSD function derived from the accelerations recorded by the transducer mounted at the shake table platform for both investigated cases; Figure 13 reports the cumulative average maximum acceleration with respect to the number of simulations for both single structure and structure coupled by ViBa; it is worth noting that these curves become stable after around 15 realizations indicating the convergence of results of the Monte Carlo Simulations.

In Figure 14 the average PSD functions of the recorded response acceleration for both cases with and without the protection of the ViBa are reported. The PSD function obtained for the case with the coupling of the structure with the ViBa shows a significant alteration of the dynamic characteristics of the global system and a reduction of the energy related to the uncoupled case. Similar behaviour has been observed in the numerical analyses as shown in Figure 7. By the comparison with the numerical results it has been also observed an increment of the energy dissipation from $\eta = 0.09$ (uncoupled case) to $\eta = 0.12$ (coupled case). Finally, Figure 15 shows the results in terms of cumulative average reduction factor. It is worth mentioning that each individual RF obtained from each individual experiment is less than unity which means that the ViBa always provides a beneficial effect for every single case; the results range from the highest reduction of about 42% (RF=0.584) to a minimum of 9% (RF=0.914) and with an average value of 26% corresponding to RF equal to 0.743 close to the value evaluated from the optimization procedure and from the numerical results obtained from a power spectral analysis performed in SAP2000 (RF = 0.72).

6 CONCLUSIONS

A novel vibration control strategy has been proposed in this paper to reduce the vibrations of structure due to seismic waves. The new strategy exploits the structure-soil-structure interaction mechanism to develop a novel device herein called Vibrating Barrier (ViBa). This barrier is hosted in the soil nearby the structure to be protected and it is designed to absorb part of the seismic input. Remarkably the device is not in contact with the structure, therefore can be used to protect existing structures. A simplified structural model has been used design the ViBa device. Specifically, a cantilevered structure founded on monopile has been selected as the structure to be protected; the ViBa has been modelled as well as a cantilevered structure founded on monopile. Numerical and experimental tests have been carried out to explore the effectiveness of the ViBa in reducing the vibration of a simplified structure. Various soil conditions according to the Eurocode 8 classification

have been considered in the numerical model highlighting the effectiveness of the ViBa for different different scenarios. Interestingly a reduction of up to 44% has been achieved. Experimental results did validate the numerical model adopted. The paper represents the first study in this field and addressed the design of this innovative device through a simplified approach. The study provides a framework to enhance the modelling by including nonlinear behaviour in soil and structures as well as non-stationary spatially variable ground motion models. Moreover, it is worth noting that as the ViBa is hosted in the soil it can be able protect more than one structure according to the Poulos's superposition procedure [30]. Specifically, the response of a pile groups can be obtained from the study of only two piles at a time by assuming "transparent" the other piles. As proven by several authors (see e.g Roesset [31], Kaynia and Kausel [32]), the results of this approximation are in very good agreement with more rigorous dynamic solutions as the pile diameter is small in comparison to the seismic wavelength.

ACKNOWLEDGMENTS

This research was supported by the EPSRC First Grant EP/K004867/1 "Vibrating Barriers for the control of seismic waves (ViBa)".

REFERENCES

[1] Woods RD. Screening of surface waves in soils. J. Soil Mech. Found. Eng. Div. ASCE; 1968,94 (4):951–979.

[2] Warburton GB, Richardson JD, Webster JJ. Forced Vibrations of Two Masses on an Elastic Half Space. Journal of Applied Mechanics. 1971;38(1):148.

[3] Luco JE, Contesse L. Dynamic structure–soil–structure interaction. Bulletin of the Seismological Society of America 1973;63(4):1289–303.

[4] Kobori T, Kusakabe K, Cross-interaction between two embedded structures in earthquakes. In: Proceedings of the seventh world conference on earth- quake engineering. Istanbul, Turkey, 1980; p. 65–72.

[5] Mulliken JS, Karabalis DL. Discrete model for dynamic through-the-soil coupling of 3-D foundations and structures. Earthquake Engineering & Structural Dynamics. 1998 Jul;27(7):687–710.

[6] Naserkhaki S, Pourmohammad H. SSI and SSSI effects in seismic analysis of twin buildings: discrete model concept. Journal of Civil Engineering and Management. 2012 Dec;18(6):890–8.

[7] Menglin L, Huaifeng W, Xi C, Yongmei Z. Structure–soil–structure interaction: Literature review, Soil Dynamics and Earthquake Engineering. 31 1724–1731, 2011.

[8] Clouteau D, Aubry D. Modifications of the ground motion in dense urban areas, Journal of Computational Acoustics; 9, 1659-1675, 2001.

[9] Chávez-García FJ, Cárdenas-Soto M. The contribution of the built environment to the free-field ground motion in Mexico city, Soil Dyn. Earthq. Eng.; 22, 773-780, 2002.

[10] Kham M, Semblat J-F, Bard P-Y, Dangla P. Seismic site-city interaction: main governing phenomena through simplified numerical models, Bull. Seism. Soc. Am. 2006; 96, no.5, 1934-1951.

[11] Guéguen P, Bard P-Y, Chavez-Garcia FJ. Site-City Interaction in Mexico City-Like environments: An Analytical Study. Bull. Seism. Soc. Am. 2002; 92,2, 794-811.

[12] Boutin C, Roussillon P. Assessment of the urbanization effect on seismic response. Bull. Seism. Soc. Am 2004; 94(1), 251-268.

[13] Behnamfar F, Sugimura Y. Dynamic response of adjacent structures under spatially variable seismic waves. Probabilistic Engineering Mechanics 1999; 14:33-44.

[14] Alexander NA, Ibraim E, Aldaikh H. Exploration of Structure-Soil-Structure Interaction Dynamics. Proceedings of the Thirteenth International Conference on Civil, Structural and Environmental Engineering Computing, B.H.V. Topping and Y. Tsompanakis, (Editors), Civil-Comp Press, Stirlingshire, United Kingdom, paper 216; 2011.

[15] Dobry R, Gazetas G. Simple method for dynamic stiffness and damping of floating pile groups. Geotechnique 1988; London 38:557 – 574.

[16] Mylonakis G, Gazetas G. Lateral Vibration and Internal Forces of Grouped Piles in Layered Soil. Journal of Geotechnical and Geoenvironmental Engineering 1999 ; 125:16–25.

[17] Makris N, Gazetas G. Dynamic pile-soil-pile interaction. Part II: Lateral and seismic response. Earthquake Engineering & Structural Dynamics 1992; 21:145–162.

[18] Dezi F, Carbonari S, Leoni G. A model for the 3D kinematic interaction analysis of pile groups in layered soils. Earthquake Engineering & Structural Dynamics 2009; 38:1281–1305.

[19] Kimball A, Lovell D. Internal Friction in Solids. Physical Review 1927; 30(6):948–59.

[20] Novak M. Dynamic Stiffness and Damping of Piles. Canadian Geotechnical Journal 1974; 11(4):574–98.

[21] Morse PM, Ingard KU. Theoretical Acoustics. Princeton University Press. Princeton, New Jersey; 1968.

[22] Vanmarcke EH. Properties of spectral moments with applications to random vibration. J. Eng. Mech. 1972; 98(2):425–446.

[23] Commission of European Communities, Eurocode 8, earthquake resistant design of structures, Brussels, Belgium, 1998.

[24] Cacciola P, Colajanni P, Muscolino G. Combination of modal responses consistent with seismic input representation. Journal of Structural Engineering 2004; 30(1):47-55.

[25] Padrón LA, Aznárez JJ, Maeso O. Dynamic structure–soil–structure interaction between nearby piled buildings under seismic excitation by BEM–FEM model. Soil Dynamics and Earthquake Engineering. 2009 Jun;29(6):1084–96.

[26] Kitada Y, Hirotani T, Iguchi M. Models test on dynamic structure–structure interaction of nuclear power plant buildings. Nuclear Engineering and Design. 1999 Sep;192(2-3):205–16.

[27] Clouteau D, Broc D, Devésa G, Guyonvarh V, Massin P. Calculation methods of Structure–Soil–Structure Interaction (3SI) for embedded buildings: Application to NUPEC tests. Soil Dynamics and Earthquake Engineering. 2012 Jan;32(1):129–42.

[28] Niwa, M., Ueno, K., Yahata, K., Ishibashi, T.. Vibration tests of soil-structure interaction using silicone rubber soil model, in: Ninth World Conference on Earthquake Engineering. Tokyo-Kyoto, Japan, 1988.

[29] Computer and Structures. CSI analysis reference manual. SAP 2000, Berkeley (CA), 2005.

[30] Poulos HG. Behavior of laterally-loaded piles II: pile groups. Journal of Soil Mechanics and Foundations Division, ASCE, 1971; 91:733-751.

[31] Roesset JM. Dynamic stiffness of pile groups. Analysis and Design of Pile Foundations, ASCE, 1984:263-286.

[32] Kaynia AM and Kausel E. Dynamic stiffness and seismic response of pile groups. Research Report R82-03. Massachusset Institute of Technology, 1982.

Table 1. Properties of the investigated soil deposits

Soil Type	V_s [m/s]	ρ_s [kg/m^3]	υ
A	800	2000	0.45
B	400	2000	0.45
C	200	2000	0.45
D	100	2000	0.45

Table 2. Comparison of the fundamental frequencies of the structure considering SSI and the soil deposit

Soil Type	f_{soil} [Hz]	f_{str} [Hz]	$\frac{(f_{soil}-f_{str})}{f_{str}}\%$
A	6.67	2.67	150
B	3.33	2.08	60.1
C	1.67	1.57	6.4
D	0.83	1.15	-28.0

Table 3 Properties of the materials used in the experimental test

Materials	**Young's Elastic Modulus [kPa]**	**Poisson coefficient**	**Unit weight [kN/m^3]**
Silicone rubber	470.66	0.47	12.29
Aluminium	69637055.00	0.33	26.60
Steel	84980000.00	0.30	76.36

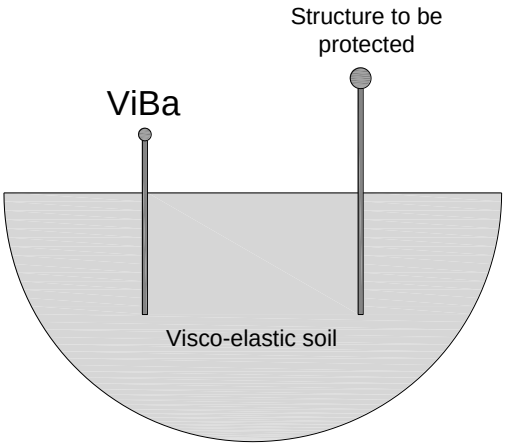

Figure 1. ViBa-soil-structure system

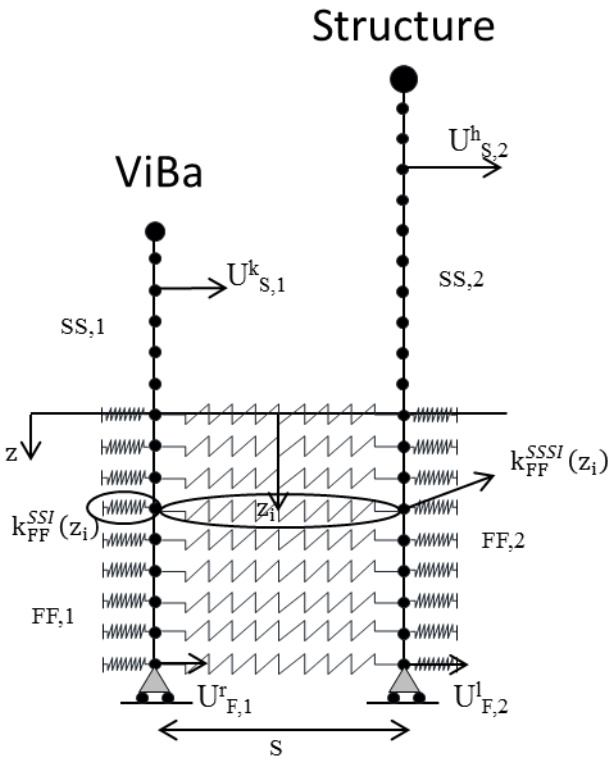

Figure 2. Discrete ViBa-soil-structure interaction model

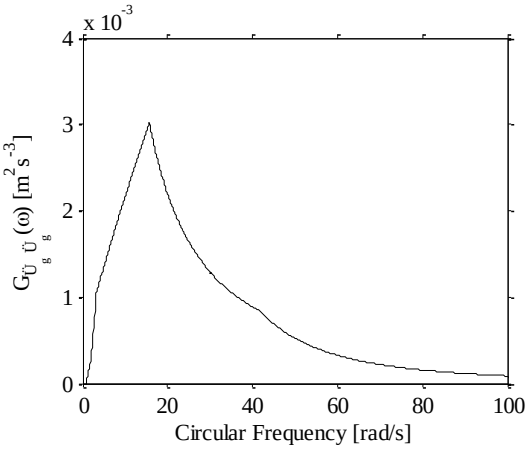

Figure 3. Input PSD defined at bedrock

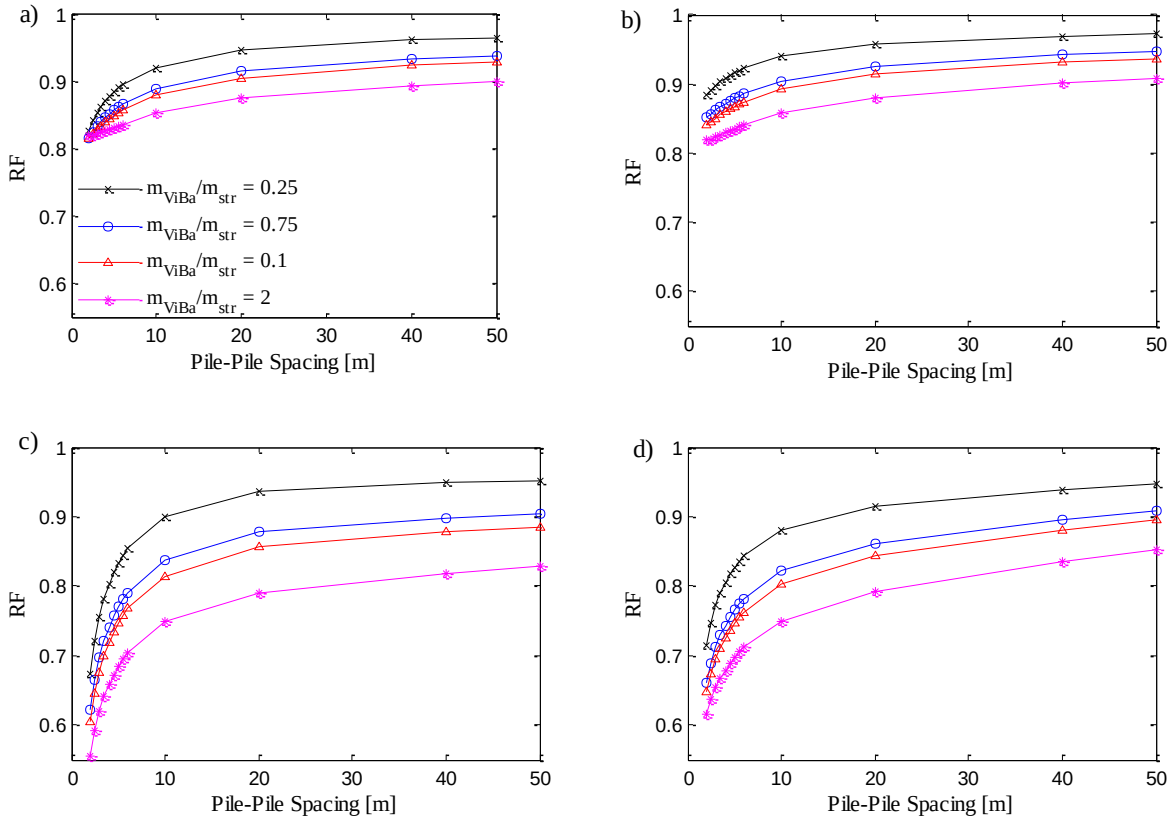

Figure 4 Reduction factor curves for soil type a) A, b) B, c) C, and d) D

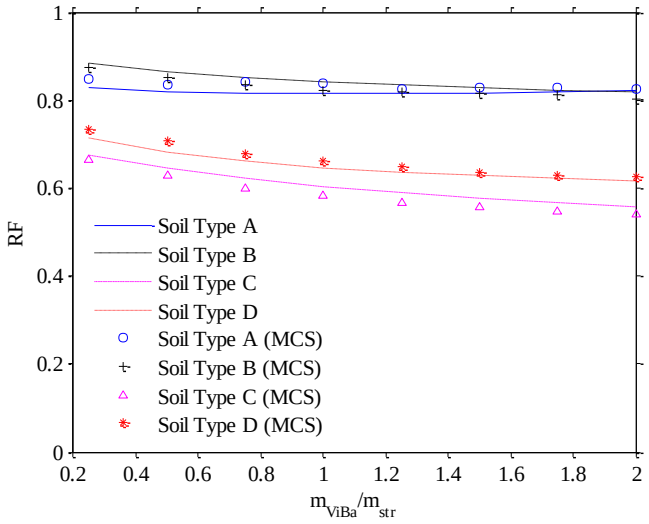

Figure 5. RF curves obtained for several soil types after tuning the ViBa for spacing = 1 m

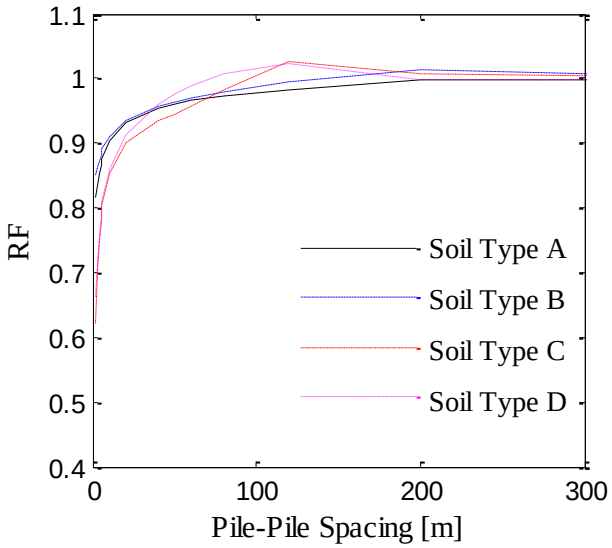

Figure 6. RF values at several distances after tuning the ViBa for spacing = 1 m

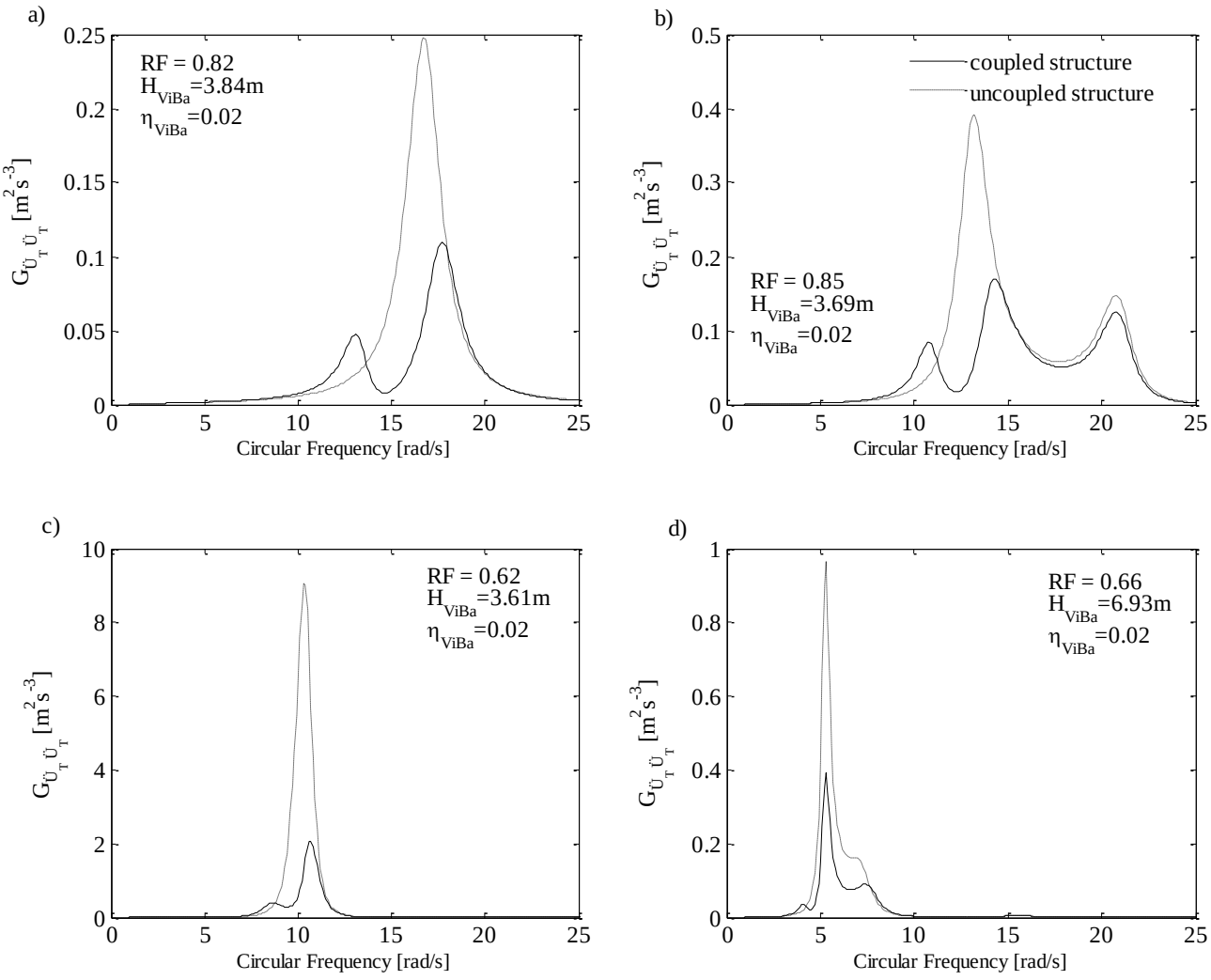

Figure 7. Acceleration PSD functions for soil type a) A, b) B, c) C, and d) D obtained for mass ratio = 0.75 and spacing = 1m

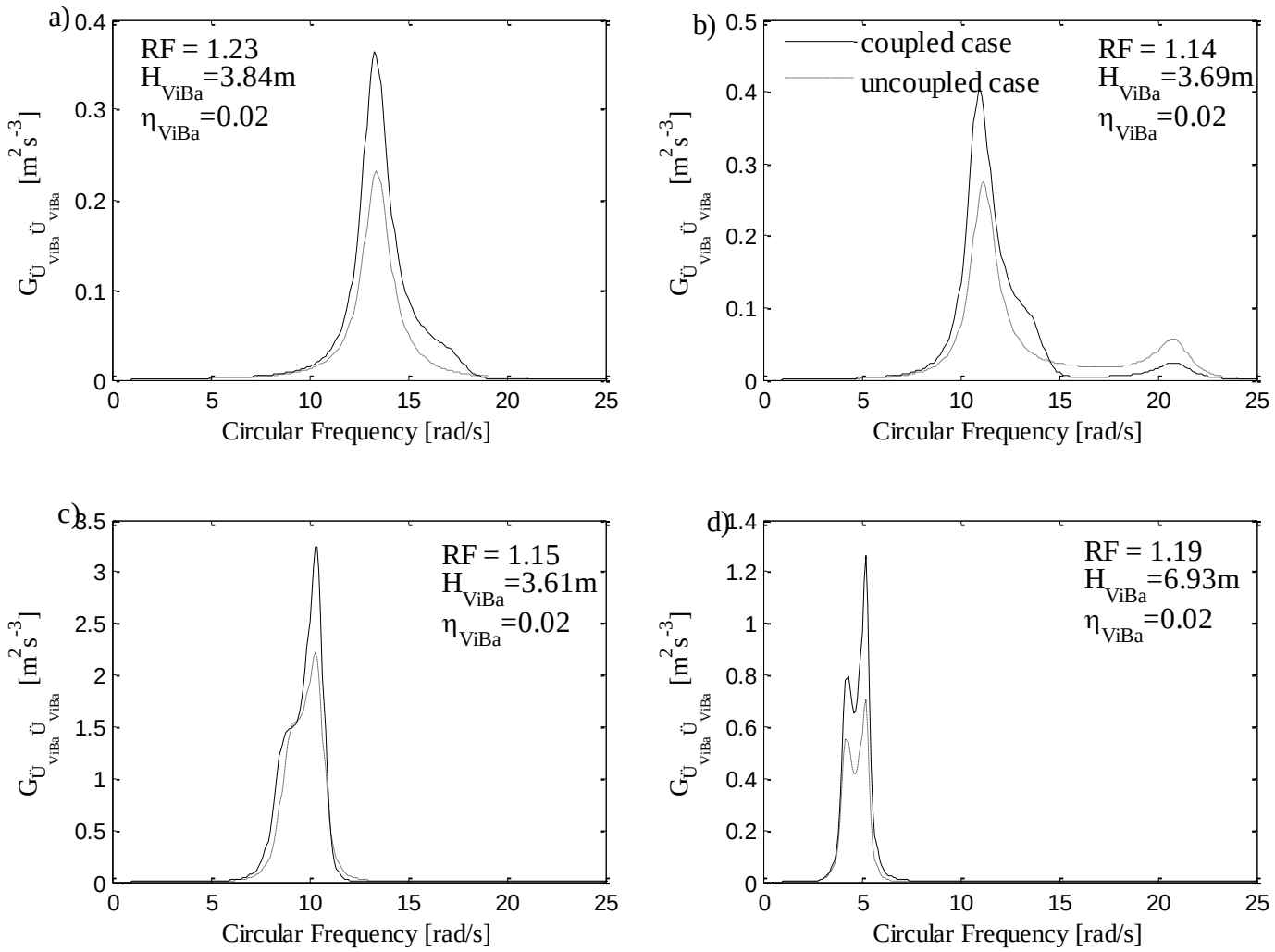

Figure 8 Acceleration PSD functions of the ViBa for soil type a) A, b) B, c) C, and d) D obtained for mass ratio = 0.75 and spacing = 1m

a) b)

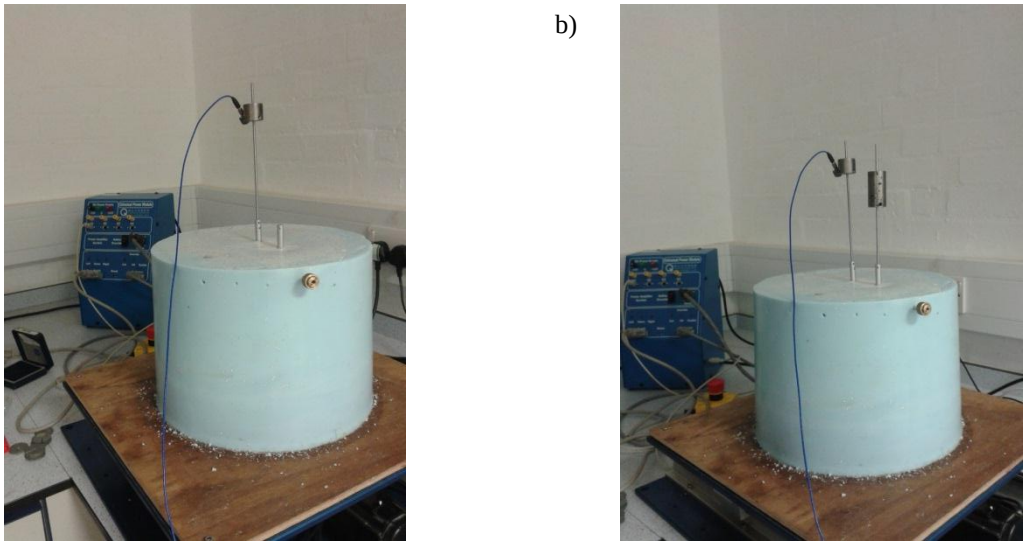

Figure 9 Test models realized in the laboratory and placed over a shaking table for a)single structure and b)structure coupled with ViBa.

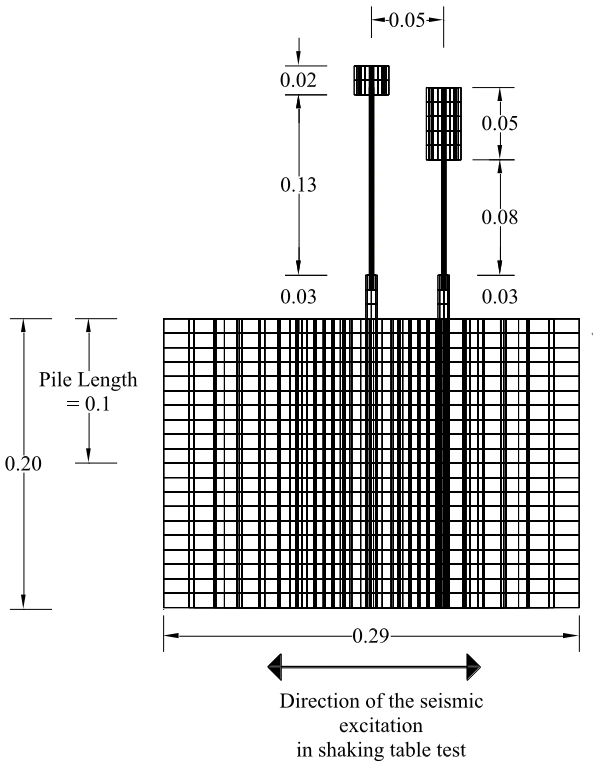

Figure 10 Set up of the experiment for shaking table (case with structure protected by ViBa device)

a) b)

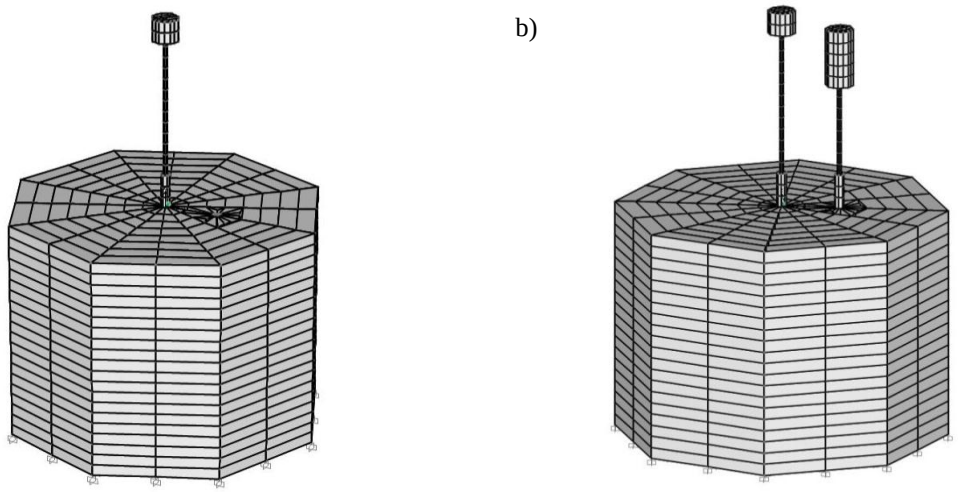

Figure 11 Reproduction of the experimental test by SAP2000 for both cases: a) without and b) with the protection by ViBa

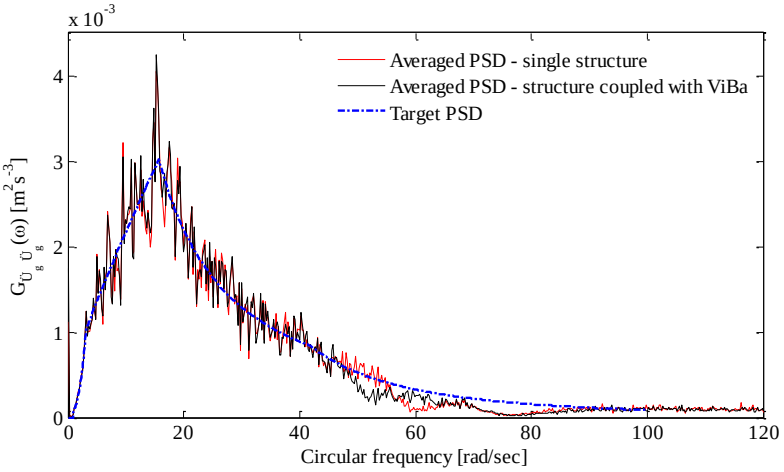

Figure 12 Comparison between desired and measured Power Spectral Density curves at the shake table platform

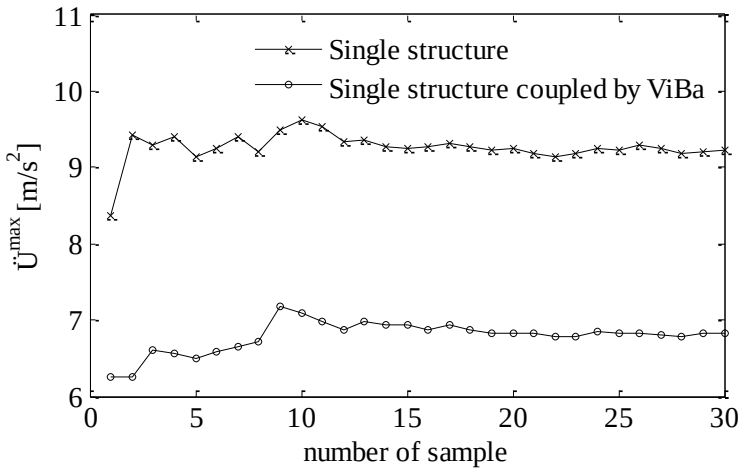

Figure 13 Cumulative average of the recorded maximum accelerations of the structure for single structure and structure coupled by ViBa

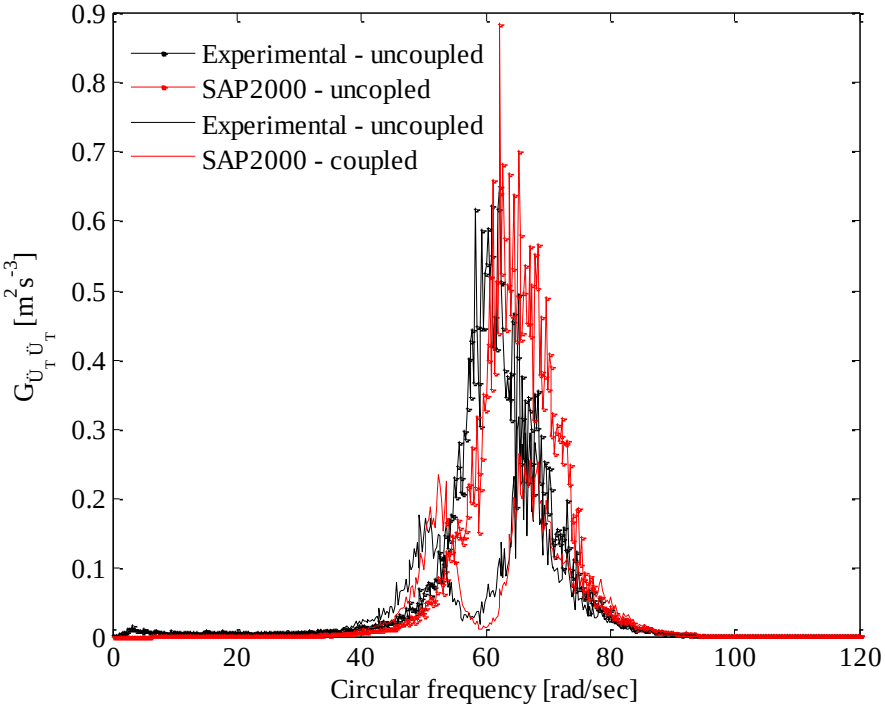

Figure 14 Numerical and experimental averaged power spectral density functions of the recorded accelerograms of the structure without and with the coupling of the ViBa

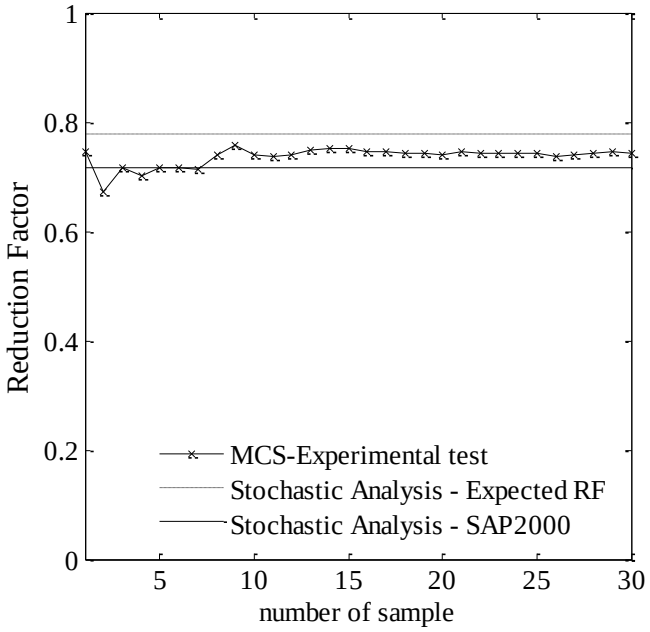

Figure 15 Evaluation of cumulative reduction factor in MCS and comparison with results from stochastic analyses